

First-order metal-insulator transition and spin-polarized tunneling in Fe_3O_4 nanocrystals

Pankaj Poddar, Tcipi Fried, and Gil Markovich*

School of Chemistry, Tel Aviv University, Tel Aviv 69978, Israel

(Received 4 February 2002; published 16 April 2002)

Tunneling junctions of stacked monolayers of uniform, organically functionalized Fe_3O_4 nanocrystals of 5.5 nm average diameter were prepared. Current-voltage characteristics of the junctions were studied as function of temperature and magnetic field. An abrupt increase in the resistance was observed on cooling below 96 K. This is attributed to the Verwey metal-insulator transition in the nanocrystals. Above 96 K, the I - V curves reflect the density of states of the narrow conduction band. This conductance peak is sensitive to the external magnetic field and exhibits large magnetoresistance.

DOI: 10.1103/PhysRevB.65.172405

PACS number(s): 75.75.+a, 85.75.Mm, 85.75.Ss

Studies of phase transitions in finite solid systems such as atomic and molecular clusters isolated in molecular beams,^{1,2} and their condensed phase counterparts, the surface-passivated nanocrystals,^{3,4} are of major importance for the understanding of fundamental physical properties of solids. To date, pressure-induced structural phase transitions in semiconductor nanocrystals were thoroughly studied by Wickham *et al.*⁵ and Lu *et al.*⁶ Other materials, such as rare-earth and transition-metal oxides, which often exhibit strong electronic and magnetic phase transitions as functions of temperature,⁷ are good candidates for studying electronic phase transitions in finite systems.

One of the most thoroughly studied electronic phase transitions is the Verwey transition observed in magnetite (Fe_3O_4).⁸ Magnetite is a relatively good conductor at room temperature, and on cooling below 120 K its conductivity drops by two orders of magnitude. It was described as a first-order metal-insulator (MI) transition accompanied by a structural phase transition where the cubic symmetry of the Fe_3O_4 crystal is broken by a small lattice distortion.⁹ While the exact nature of the transition is still under controversy, it is understood that the driving force for this phenomenon is the strong electron-electron and electron-lattice interactions in the system.

In this report, we present evidence of the existence of a temperature-induced first-order MI transition in well-separated magnetite (Fe_3O_4) nanocrystals of 5.5 nm average diameter. This transition is related to the Verwey transition observed for bulk magnetite crystals.

Recently, indications of the occurrence of the Verwey transition in nanocrystalline magnetite thin films¹⁰ and in highly nonstoichiometric nanometric powders¹¹ were found using magnetic susceptibility measurements, but without the accompanying conductivity changes. In well-separated Fe_3O_4 nanocrystals, numerous magnetic measurements did not detect this transition.¹² The electronic structure of isolated magnetite nanocrystals was not explored at low temperatures.

The conductivity of magnetite arises from charge transfer (or delocalization) between equivalent Fe^{2+} and Fe^{3+} sites and the drop in conductivity at the transition temperature (T_v) is due to localization of the extra valence electrons. It is disputed whether above T_v the material behaves as a semi-metal with a finite density of delocalized states at the Fermi level,¹³ or as a semiconductor with a small band gap¹⁴ with

some activation energy associated with the excitation of charge carriers which may be weakly trapped. Considering the insulating phase, some experimental data indicated that the insulating state is a Wigner crystal,^{15,16} i.e., it is an ordered localized charge phase, though recent resonant x-ray scattering,¹⁷ high-pressure conductivity¹³ and NMR (Ref. 18) results did not find charge ordering in the insulating phase.

Electron tunneling spectroscopy of magnetite nanocrystals of varying sizes has the potential of clarifying these issues. Resonant tunneling of electrons through the electronic levels of isolated organically passivated nanocrystals was found to be insensitive to grain boundary effects (surface states) in scanning tunneling microscopy (STM) experiments,¹⁹ while such boundaries have a major contribution to long-range electron transport through polycrystalline thin films. We have thus chosen this approach to study electron tunneling through relatively homogeneous, separated magnetite nanocrystal arrays. Previous studies of electron tunneling at bulk magnetite surfaces using STM (Refs. 20 and 21) have provided valuable information on the electronic structure of the material's surface, but without a clear correspondence with the bulk's interior states.

A pioneering work by Black *et al.*²² has recently shown that self-assembled devices composed of 10-nm colloidal Co nanocrystals display spin-dependent electron transport, with a magnetoresistance (MR) of 10% below 20 K. Electron transport properties of magnetite nanocrystal arrays should be influenced by its ferrimagnetic properties. Magnetite represents a family of materials which fall into the category of half-metals,²³ where the electronic density of states is spin polarized at the Fermi level, and the conductivity is dominated by these spin-polarized charge carriers. In spite of its promising properties, most studies of spin-polarized electron conduction in magnetite in the form of single crystals, polycrystalline powders, and thin epitaxial films²⁴ did not observe large MR effects.

In this study, arrays of magnetite nanocrystals separated by the fatty acid molecules adsorbed to their surfaces were deposited in vertical tunneling junctions between gold electrodes using the Langmuir-Blodgett technique.²⁵ The current-voltage characteristics of the junctions were measured as a function of temperature and magnetic field.

The details of magnetite nanoparticle array preparation are described elsewhere.²⁶ In brief, for Fe_3O_4 nanoparticle synthesis, a mixture of Fe^{2+} and Fe^{3+} (1:2 molar ratio) (Ref. 27) in an aqueous medium is treated with ammonia at elevated temperature—typically 80 °C in an inert atmosphere,

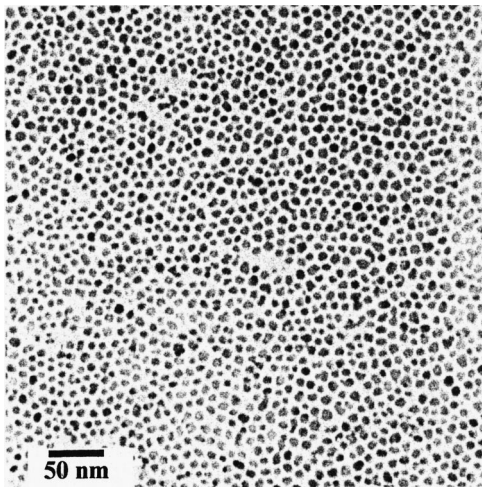


FIG. 1. TEM image of the Fe_3O_4 nanoparticle monolayer.

followed by encapsulating the resulting nanoparticles with oleic acid. The particles are neutralized, dispersed in nonpolar organic solvents, and separated by employing size-selective precipitation to produce uniform samples in the 3–10 nm size range. Transmission electron microscopy (TEM) was used for size determination as well as to confirm the formation of nanoparticle monolayers by transferring the Langmuir-Blodgett (LB) films on carbon coated TEM grid. The LB films are produced by depositing the hydrophobic magnetite nanocrystals from heptane solution at the air-water interface and compressing the film two-dimensionally to form a close-packed array. A TEM image of an array used for the present study (Fig. 1) shows a monolayer of particles with average core diameter of 5.5 ± 1.4 nm. We heated a TEM grid with a particle film at 250°C for 3 h in vacuum to check the stability of the array. The TEM image showed that after this treatment the particles were well separated and maintained their individual single-crystal structure without forming aggregates.

Powder x-ray studies confirmed the presence of magnetite inverse spinel structure. As additional tests to verify the presence of Fe_3O_4 rather than maghemite ($\gamma\text{-Fe}_2\text{O}_3$) which has an almost identical diffraction pattern, x-ray photoelectron spectroscopy was used to roughly check the Fe:O stoichiometry and near-IR absorption was used to detect an absorption feature at about 7000 cm^{-1} which is unique to magnetite. For the fabrication of the junctions, arrays of gold lines (width = $80\ \mu\text{m}$) and a thickness of 100 nm were deposited on a doped Si(100) substrate with a 1000-Å-thick oxide layer. Consequently, five monolayers of Fe_3O_4 nanocrystals were transferred on the patterned substrates using the Langmuir-Schafer technique.²⁶ A second array of gold lines perpendicular to the bottom electrodes was deposited by thermal evaporation through a shadow mask on top of the films while the substrates were maintained at 20°C . The electrical contacts were made by fixing a Cu wire to pads on the gold electrodes using silver paste. The low contact resistance was verified by connecting two copper wires to each gold electrode and checking for the resistance. The samples were mounted in a closed cycle helium cryostat. Current-voltage (I - V) characteristics were recorded down to 10 K with and

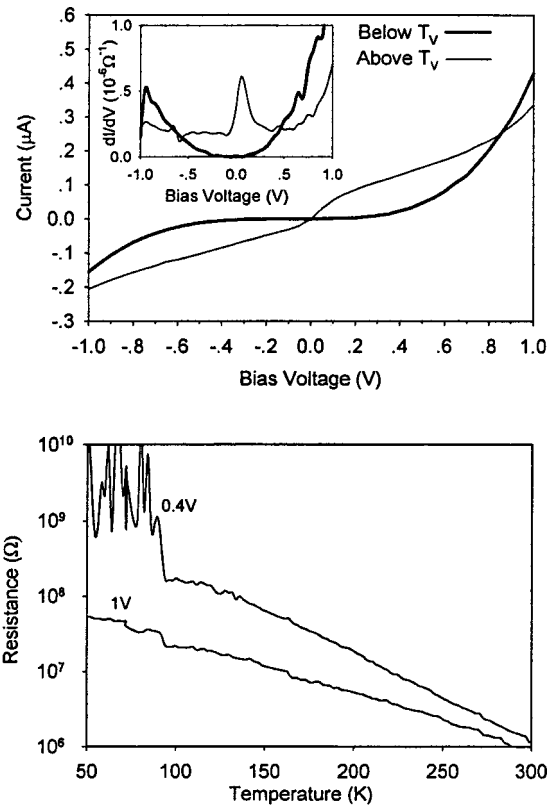


FIG. 2. Top: I - V curves below and above the Verwey transition temperature. Inset: derivative (differential conductivity) of these curves. Bottom: junction resistance as function of temperature for two bias voltage values.

without application of magnetic field (up to 4 kOe) parallel to the plane of the film. Device resistance was sensitive to the amount of excess oleic acid present in the LB films. For the present study, relatively good conduction between the deposited layers was needed. Hence, low resistance devices with typical room temperature resistance of about 4–10 M Ω were used.

The macroscopic tunneling junctions are perceived as consisting of parallel percolating current paths, where each path may include several interparticle junctions. Hence, the details of the current-voltage curves are determined not only by the single-particle electronic structure but also by the RC constants of the various inter-particle tunneling junctions in the current paths. In Fig. 2 (top), it is observed that the I - V curves of a typical junction significantly change on cooling below 100 K. This change was reversible and reproducible through several cooling-heating cycles. In Fig. 2 (bottom), a sharp resistance jump is observed at 96 ± 2 K. Since RC characteristics of the junctions are not sensitive to temperature, we believe that this abrupt change in electronic structure of the sample is a manifestation of the single-particle MI transition. As commonly accepted, the sharp jump (discontinuity) in junction resistance as function of temperature indicates a first-order phase transition.¹⁶

It appears that in the metallic phase (above 96 K), the large slope of the I - V curve around zero bias voltage (the Fermi level) reflects the narrow conduction band of magne-

tite, similar to the observations in low temperature STM studies of the bulk surface.²¹ Below 96 K the low conductance plateau corresponds with low density of states around the Fermi level of the nanocrystals and its width is determined by interparticle junction parameters.

It is interesting to compare the numerous reports on the Verwey transition in different forms of bulk magnetite such as single crystals, thin epitaxial films, and polycrystalline powders to the present study. It is commonly observed that the transition temperature decreases with increasing deviations from ideal Fe:O stoichiometry of less than 0.3%. With larger deviations, the transition changes to second order, and finally disappears altogether at about 1% deviation.^{28,29} In thin polycrystalline films, the transition did not appear in conductivity measurements, while a change in magnetic susceptibility indicated the occurrence of a phase transition.^{30,31} In the present study, the isolated small nanocrystals have a large surface-to-volume ratio and probable off-stoichiometry at the surface. Yet, surprisingly, the MI transition in the nanocrystals appears very sharp, and the change in conductance at low bias voltages extends over several orders of magnitude.

In all measurements on polycrystalline materials the electrode separation was macroscopic, and electron transport was susceptible to various trapping and scattering processes, washing out interesting features from the measurement results. In the present study, electrons travel over a short distance by tunneling through several isolated particles, thus allowing a relatively large number of electrons to pass between the electrodes without trapping.

The change in the density of states of the nanocrystals, compared with the bulk and possible quantum confinement effects, may contribute to the large conductance jump measured at T_v . A theoretical investigation would provide information about the influence of finite-size effects on the band structure, and thus its affect on the interplay between stoichiometry and particle size. The large surface-to-volume ratio may be the reason for the shift of the nanocrystal T_v (96 K) lower than the bulk value (121 K), although the existence of a sharp transition, extending over less than 5 K, in spite of the 25% particle size distribution hints that T_v is not very sensitive to particle size. Differences between the nanocrystal results and previous experiments may also originate in the preparation method: Colloidal nanocrystals are often perfect single crystals, which can easily anneal out many types of defects, while the bulk materials may contain larger amounts of trapped defects. Indeed, high-resolution TEM images confirmed that the vast majority of the particles produced in this study were perfect single crystals.

Zero-field-cooled magnetization measurements of nanoparticle monolayers on highly oriented pyrolytic graphite substrates at low magnetic field (10 Oe) did not show any evidence of a first-order transition. This is probably due to the larger magnetization effects arising from the superparamagnetic nature of the particles, compared with the expected change in magnetic susceptibility at T_v , and/or due to the large contribution of the particle surfaces to the magnetization signal.

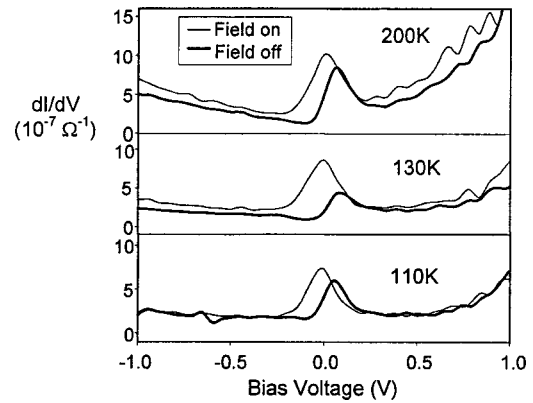


FIG. 3. dI/dV curves at three temperatures with and without a magnetic field (2.5 KOe) applied parallel to the film. Below T_v the magnetic-field effect vanishes.

The present study seems to be in agreement with recent results, which rule out a change from short- to long-range charge ordering below T_v as the transition mechanism.¹⁷ It is not likely that the abrupt change in the $I-V$ curves in such small nanocrystals, which are only several unit cells wide, could be explained based on short-range versus long-range charge ordering. In the present study, it appears that the transition is a true change from delocalized conduction electrons to localized charge carriers in an insulating material.

In Fig. 3, the magnetic-field influence on the differential conductance (dI/dV) vs bias voltage curves at 200, 130, and 110 K is presented. Figure 4 has the relative MR at a -5 mV bias voltage, based on measured dc resistance values, plotted as function of temperature. A large negative MR increasing down to T_v is observed, while below T_v no significant MR was detected at low bias voltage. The data were taken with a field of 2.5 kOe parallel to the film plane, which is close to the saturation of the MR effect. The dI/dV curves show a peak around the Fermi level, which is proportional to the density of states. In the presence of a magnetic field the peak height and width increase. The temperature dependence of the MR in Fig. 4 should be taken with caution because of the highly nonlinear form of the current-voltage curves. A comparison of the relative increase in the differential conduc-

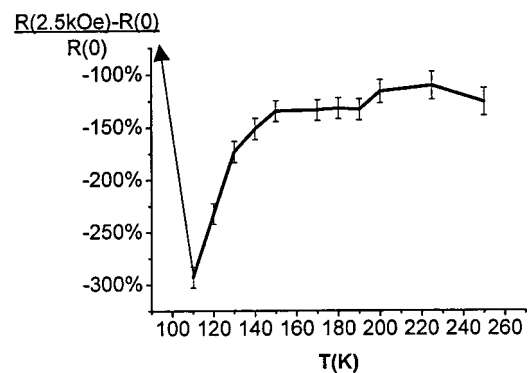


FIG. 4. Magnetoresistance as function of the temperature, measured at a -5 mV bias voltage. The temperature dependence of the MR below 200 K is sensitive to the low-bias value used in the measurement.

tance peak with application of magnetic field shows that it reaches a maximum around 130 K and then decreases towards T_V (Fig. 3).

External magnetic field affects the electron transport through an alignment of the magnetic moments of the superparamagnetic nanocrystals in a preferred direction. This increases the probability of electrons to tunnel between the spin-polarized conduction bands of adjacent nanocrystals. Decreasing the temperature improves the alignment according to the Curie-Weiss law down to the blocking temperature of the nanocrystals, where their magnetic moments become trapped along their easy magnetization axis or along other orientations dictated by the strong dipolar interactions with their neighbors. Isolated 5.5 nm magnetite nanocrystals have a blocking temperature well below 100 K.²⁶ The subpopulation of nanocrystals, which contribute to the conductance of the junctions, must be strongly coupled and therefore has a higher blocking temperature. This effect can explain a decrease in the magnetic-field influence on the differential conductance peak below 130 K. Decreasing the temperature could also increase the degree of spin polarization near the Fermi level, hence contributing to an increase in the MR.

The large magnetic-field influence on the differential con-

ductance peak is strong evidence that the measured I - V curves reflect the electronic structure of the nanocrystals. The large negative MR measured at low temperatures ($\sim 300\%$) is higher than bulk magnetite MR ($\sim 4\%$ up to 70% at T_V under a high field) (Ref. 32) or polycrystalline films ($\sim 3\%$).^{30,31} Spin valve devices, in which electrons tunnel through a Fe_3O_4 thin film separated by a thin oxide insulator,^{33,34} are comparable to the nanocrystal tunneling junctions. Such devices have typically shown larger MR effects (30–40%, low field), although still smaller than the effect observed in this work, possibly due to the lower sensitivity of the tunneling in the nanocrystals to surface states and/or the superparamagnetism of the particles.

This study of magnetotransport in nanometric iron-ferrite crystals around the Verwey transition holds promise for a better understanding of such solid-state systems. Combined with theoretical investigations, it will serve as a good model system to study the size dependence of electronic/structural phase transitions, and to describe such transitions in other materials.

This work was supported by The Israel Science Foundation and by the Israeli Ministry of Science.

*Corresponding author. Email address: gilmar@post.tau.ac.il

¹M. Schmidt, R. Kusche, T. Hippler, J. Donges, W. Kronmüller, B. Issendorff, and H. Haberland, *Phys. Rev. Lett.* **86**, 1191 (2001).

²C. Molteni, R. Martonak, and M. Parrinello, *J. Chem. Phys.* **12**, 5358 (2001).

³K. Jacobs, D. Zaziski, E. C. Scher, A. B. Herhold, and A. P. Alivisatos, *Science* **293**, 1803 (2001).

⁴S. B. Qadri, E. F. Skelton, D. Hsu, A. D. Dinsmore, J. Yang, H. F. Gray, and B. R. Ratna, *Phys. Rev. B* **60**, 9191 (1999).

⁵J. N. Wickham, A. B. Herhold, and A. P. Alivisatos, *Phys. Rev. Lett.* **84**, 923 (2000).

⁶J. S. Lu, Q. Cui, H. Yang, B. Liu, and G. Zou, *Mater. Lett.* **41**, 97 (1999).

⁷C. N. R. Rao, *J. Mater. Chem.* **9**, 1 (1999).

⁸E. J. W. Verwey, *Nature (London)* **144**, 327 (1939).

⁹M. Izumi, T. F. Koetzle, G. Shirane, S. Chikazumi, M. Matsui, and S. Todo, *Acta Crystallogr., Sect. B: Struct. Sci.* **38**, 2121 (1982).

¹⁰J. Tang, K.-Y. Wang, and W. Zhou, *J. Appl. Phys.* **89**, 7690 (2001).

¹¹N. Guigue-Millot, N. Keller, and P. Perriat, *Phys. Rev. B* **64**, 012402 (2001).

¹²For example: W. Luo, S. R. Nagel, T. F. Rosenbaum, and R. E. Rosensweig, *Phys. Rev. Lett.* **67**, 2721 (1991).

¹³S. Todo, N. Takeshita, T. Kanehara, T. Mori, and N. Mori, *J. Appl. Phys.* **89**, 7347 (2001).

¹⁴J. H. Park, L. H. Tjeng, J. W. Allen, P. Metcalf, and C. T. Chen, *Phys. Rev. B* **55**, 12 813 (1997).

¹⁵N. F. Mott, *Metal-Insulator Transition* (Taylor & Francis, London, 1974).

¹⁶G. K. Rozenberg, G. R. Hearne, M. P. Pasternak, P. A. Metcalf, and J. M. Honig, *Phys. Rev. B* **53**, 6482 (1996).

¹⁷J. Garcia, G. Subías, M. G. Proietti, J. Blasco, H. Renevier, J. L. Hodeau, and Y. Joly, *Phys. Rev. B* **63**, 054110 (2001).

¹⁸P. Novak, H. Stepánková, J. English, J. Kohou, and V. A. M. Brabers, *Phys. Rev. B* **61**, 1256 (2000).

¹⁹O. Millo, D. Katz, Y. W. Cao, and U. Banin, *Phys. Rev. B* **61**, 16 773 (2000).

²⁰R. Wiesendanger, I. V. Shevets, and J. M. D. Coey, *J. Vac. Sci. Technol. B* **12**, 2118 (1994).

²¹A. Gupta and J. Z. Sun, *J. Magn. Magn. Mater.* **200**, 24 (1999).

²²C. T. Black, C. B. Murry, R. L. Sandstorm, and Shouheng Sun, *Science* **290**, 1131 (2000).

²³J.-H. Park, E. Vescovo, H.-J. Kim, C. Kwon, R. Ramesh, and T. Venkatesan, *Nature (London)* **392**, 794 (1998).

²⁴J. M. D. Coey, A. E. Berkowitz, L. Balcells, F. F. Putris, and F. T. Parker, *Appl. Phys. Lett.* **72**, 734 (1998); X. W. Li, A. Gupta, G. Xiao, and G. Q. Gong, *J. Appl. Phys.* **83**, 7049 (1998).

²⁵G. Markovich, D. V. Leff, S. Chung, H. M. Soyey, B. Dunn, and J. R. Heath, *Appl. Phys. Lett.* **70**, 3107 (1997).

²⁶T. Fried, G. Shemer, and G. Markovich, *Adv. Mater.* **13**, 1158 (2001).

²⁷R. Massart, *IEEE Trans. Magn.* **12**, 131 (1981).

²⁸H. Kronmüller, R. Schutzenauer, and F. Waltz, *Phys. Status Solidi A* **24**, 487 (1974).

²⁹J. P. Shepherd, J. W. Koenitzer, R. Aragon, J. Spalek, and J. M. Honig, *Phys. Rev. B* **43**, 8461 (1991).

³⁰L. Wang, J. Li, W. Ding, T. Zhou, B. Liu, W. Zhong, J. Wu, and Y. Du, *J. Magn. Magn. Mater.* **207**, 111 (1999).

³¹X. W. Li, A. Gupta, G. Xiao, and G. Q. Gong, *J. Appl. Phys.* **83**, 7049 (1998).

³²M. Ziese and H. J. Blythe, *J. Phys.: Condens. Matter* **12**, 13 (2000).

³³P. J. van der Zaag, P. J. H. Bloemen, J. M. Gaines, R. M. Wolf, P. A. A. van der Heijden, R. J. M. van de Veerdonk, and W. J. M. de Jonge, *J. Magn. Magn. Mater.* **211**, 301 (2000).

³⁴P. Seneor, A. Fert, J. L. Maurice, F. Montaigne, F. Petroff, and A. Vaures, *Appl. Phys. Lett.* **74**, 4017 (1999).